IRAQI BULLETIN OF GEOLOGY AND MINING (IBGM)\
IRAQ GEOLOGICAL SURVEY (GEOSURV-IRAQ)

*IBGM (**2025**, Vol 21; Issue 2)* 573-591

STRUCTURAL CONTROL IN THE GUMAL VALLEY BASIN, N IRAQ

Mosab N. Al-Bana[1*], Ayyed Hussein Ward[1], and Najm A. Al-Karai[1]

[1] Department of Applied Geology, College of Science, Tikrit University, Tikrit, Iraq.
***** Correspondence: mosabjabber@gmail.com; Mosab Al-Bana; ORCID: 0009-0009-7991-1301

Type of the Paper (Article)
Received: 22/05/2025
Accepted: 26/10/2025
Available online: 27/12/2025

Abstract

Map matching is a key method for identifying commonalities between maps with different content. This study focuses on the Gumal Valley basin in northern Iraq, which spans two tectonic zones: the High Fold Zone in the north and the Low Fold Zone in the south. Covering an area of 935.12 km², the basin was analyzed using a structural map that was matched with topographic, geological, drainage pattern, sub-basin, lineament structure, and Active Tectonics Index (IAT) maps. The research aims to demonstrate the structural role of folds and faults in defining basin boundaries and enhancing geological and geomorphological variability. It also investigates variations in recent tectonic activity. All analyses were conducted using a 12.5-meter resolution Digital Elevation Model (DEM) and Geographic Information System (GIS) software. The results revealed a dextral strike-slip fault extending north-south through the study area. The movement of this fault caused the eastern part of the basin to advance southward due to the tectonic stress prevailing in northern Iraq. The study concluded that this north-south-oriented dextral strike-slip fault led to the displacement of the eastern part and its relative advance over the western part. This conclusion is supported by the concentration of high and medium tectonic activity in the eastern part and its decrease in the western part of the study area.

Keywords: Structure Control; Tectonic; Map Matcting; Dextral Fault; Remote Sensing & GIS

1. Introduction

Map matching is a crucial method in structural geology for demonstrating the role of surface and subsurface geological structures, such as folds and faults, in controlling the shape of the Earth's surface and its rock exposures. This process involves overlaying multiple thematic maps with a unified coordinate system and is used to analyze the distribution of lineaments and associated valleys or rock barriers. After data integration, a new set of composite maps is produced (Al-Shamaa, 1986; Al-Kraaey, 2013).

ISSN 1811-4539, EISSN 3005-3714
https://doi.org/10.59150/ibgm2102a30
IBGM: http://ibgm-iq.org/
Academic Scientific Journals: www.iasj.net

Geomorphological indicators have been developed as fundamental survey tools for identifying areas undergoing rapid tectonic deformation (Bull et al., 1977). On a regional scale, these indicators provide essential tools for identifying tectonically active areas, assessing their susceptibility to deformation, and determining their level of tectonic activity (Edward & Nicholas, 2002). Some researchers consider the Relative Tectonic Activity Index (IAT) an effective tool for evaluating geomorphological tectonic features and have combined it with landslide frequency to predict regional landslide hazards. Furthermore, the necessary data for tectonic activation equations can often be easily obtained from Digital Elevation Models and other satellite imagery (Cheng et al., 2016; Partabian et al., 2016).

This research aims to demonstrate the relationship between geological structures (folds and faults) and several key features of the basin, including its shape, drainage patterns, distribution of rock exposures, and distribution and shapes of secondary basins. The study also examines the distribution of lineament structures and the Active Tectonics Index (IAT) and their relationship to the area's topography.

The research seeks to show the structural role of folds and faults in defining basin boundaries and increasing geological and geomorphological variability. It also analyzes the density and directional variation of lineaments and changes in recent tectonic activation.

2. Geographical Location of the Study Area

The study area is located in northern Iraq, between the cities of Duhok and Mosul, within the Zagros Fold Thrust Belt. It covers an area of 935.12 km² and is geographically situated between longitudes 43°0′E and 43°45′E and latitudes 36°30′N and 37°0′N (Figure 1). The Gumal River originates from the Gara Anticline and crosses the Atrush, Sheikha, Ain Sifini, and Maqlub folds. The catchment area of the Gumal Valley includes the Gara and Swara Tika folds and the western parts of the Bekhair and Brifka folds, in addition to the Sheikhan, Ain Sifni, Mahad, and Maqlub folds.

3. Materials and Methods

To demonstrate the structural role of the study area, a structural map (fold and fault map) was initially required. Previous studies available for the region were utilized, along with a digital elevation model with a resolution of 12.5 meters. Additionally, maps were created, including topographic, geological, lineament structures, secondary basins, surface runoff network, and Active Tectonics Index (IAT) maps. Five geomorphological indicators were used (Table 1). These maps were compared with the structural map of the basin, and a composite map was produced, comprising more than three maps (Figure 2). All operations were performed using Geographic Information Systems (GIS) and Remote Sensing (RS) techniques to determine the consistency of the analysis results on the formation of the basin structure and the structural geomorphological phenomena of the region, and to understand the tectonic movements affecting the folds in the basin.

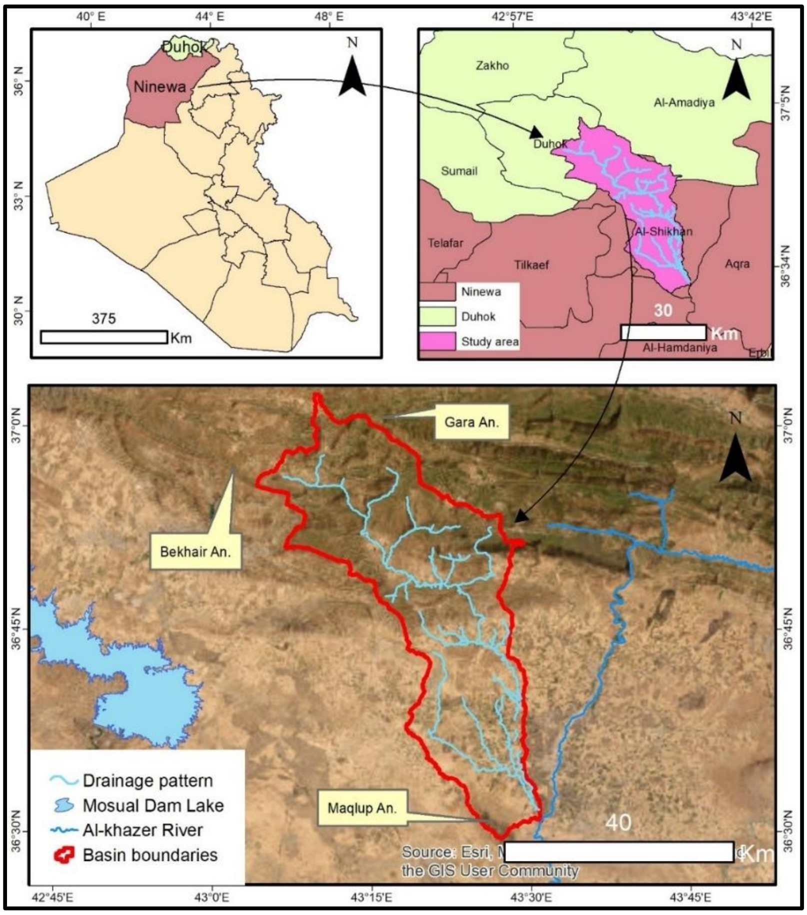

Figure 1: Location of the study area.

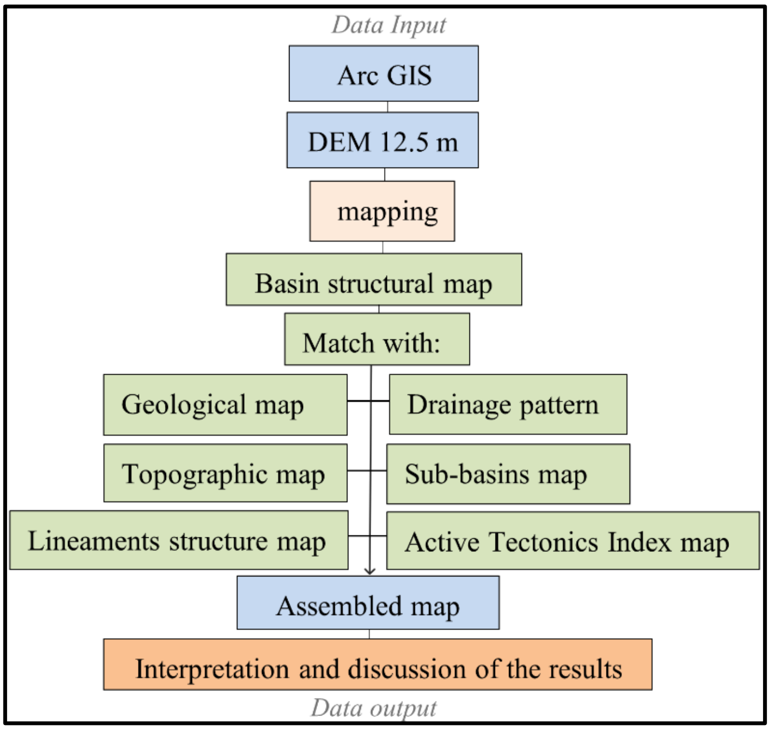

Figure 2: The methodology used in this study.

Table 1: Methodology for Calculating the Relative Tectonic Activity Index (IAT) (modified from Jeong et al., 2022).

Geomorphic indices	Mathematical derivation	Formula	Measurement procedure
Valley floor-width to height ratio, **Vf** (Bull et al.,) (1977)	$Vf = \frac{2vf_w}{(E_{ld} - E_{sc}) + (E_{rd} - E_{sc})}$	**Vf:** valley floor width to valley height ratio, **Vf_w:** valley's width (m), **E_{ld}:** left elevation (m), **E_{rd}:** right elevation (m), and **E_{sc}:** valley base elevation (m).	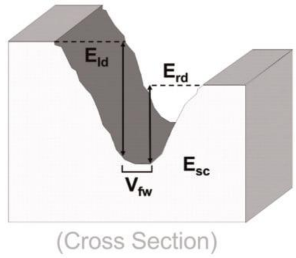
Stream length-gradient index, **SL** (Hack, 1957)	$SL = \left(\frac{\Delta H}{\Delta L}\right) * L$	**SL:** stream length gradient index, **ΔH:** Difference in Elevation (m), **ΔL:** Difference in Length (m), **L:** channel length from the divide to the midpoint of the channel reach for which the Index (m).	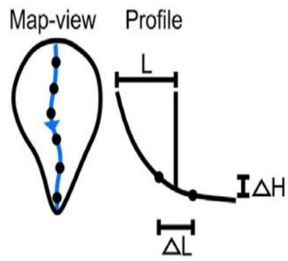
Asymmetry factor, **AF** (Edward &) Nicholas, (2002)	$AF = \left(\frac{Ar}{At}\right) * 100$	**Ar:** Area of the right of the trunk stream (km^2) and **At:** Total drainage area (km^2).	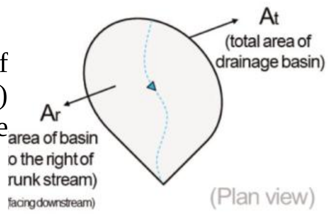
Sinuosity of mountain front, **Smf** (Bull et al., 1977)	$\boldsymbol{Smf} = \frac{L_{mf}}{L_s}$	**Smf:** Sinuosity of mountain front, **Lmf:** length of the mountain front is zigzag (km), **Ls:** Straight mountain front length (km).	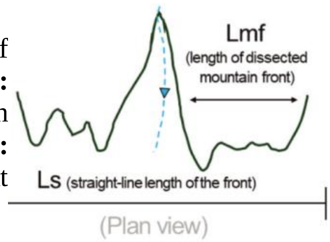
Transverse topography symmetry, **T** (Cox, 1994)	$T = \frac{D_a}{D_d}$	**T:** transverse topographic symmetry, **D_a:** deflection of the stream channel from the basin midline (km), **D_d:** distance between the basin midline and basin divide (km).	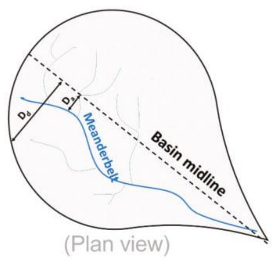
Active Tectonics Index, **IAT**	$IAT = \frac{S}{N}$	**S:** sum of the tectonic active class values **N:** number of geomorphic indices.	

4. Geological Setting

4.1. Structural geology

The study area, represented by the Gumal valley basin, includes nine anticlines distributed across the entire basin area: Maqloub, Mahad, Ain Sifni, Sheikhan, Brifka, Atrush, Swara Tika, Gara, and Bekhair anticlines. These anticlines are separated by synclinal folds, a normal result of the folding of the sedimentary cover in a wave-like pattern represented by convex and synclinal half-waves. The aforementioned anticlines are fault-related, as reverse faults determined the locations, growth, and geometry of these anticlines (Al-Azzawi, 2003). In addition to these reverse faults, most of the anticlines in the Zagros Fold Thrust Belt are affected by two systems of coupled strike-slip faults, which cut the anticlines or terminate the folding (Berberian, 1995).

The tectonics of Iraq are influenced by inherited basement block faults (NW – SE, NE – SW) extending from the Arabian Shield (Jassim & Goff, 2006). The amplification of folds and fold bends, explained by Numan & Azzawi (1993), is attributed to the tectonic reversal of movement along listric vertical faults dating back to the previous passive margin phase. The study area lies within the boundary between the Low Fold Zone and the High Fold Zone. According to Fouad (2015; Figure 3), the High Fold Zone occupies the largest part of the basin, with an area of 732.67 km², representing 78.35% of the total area.

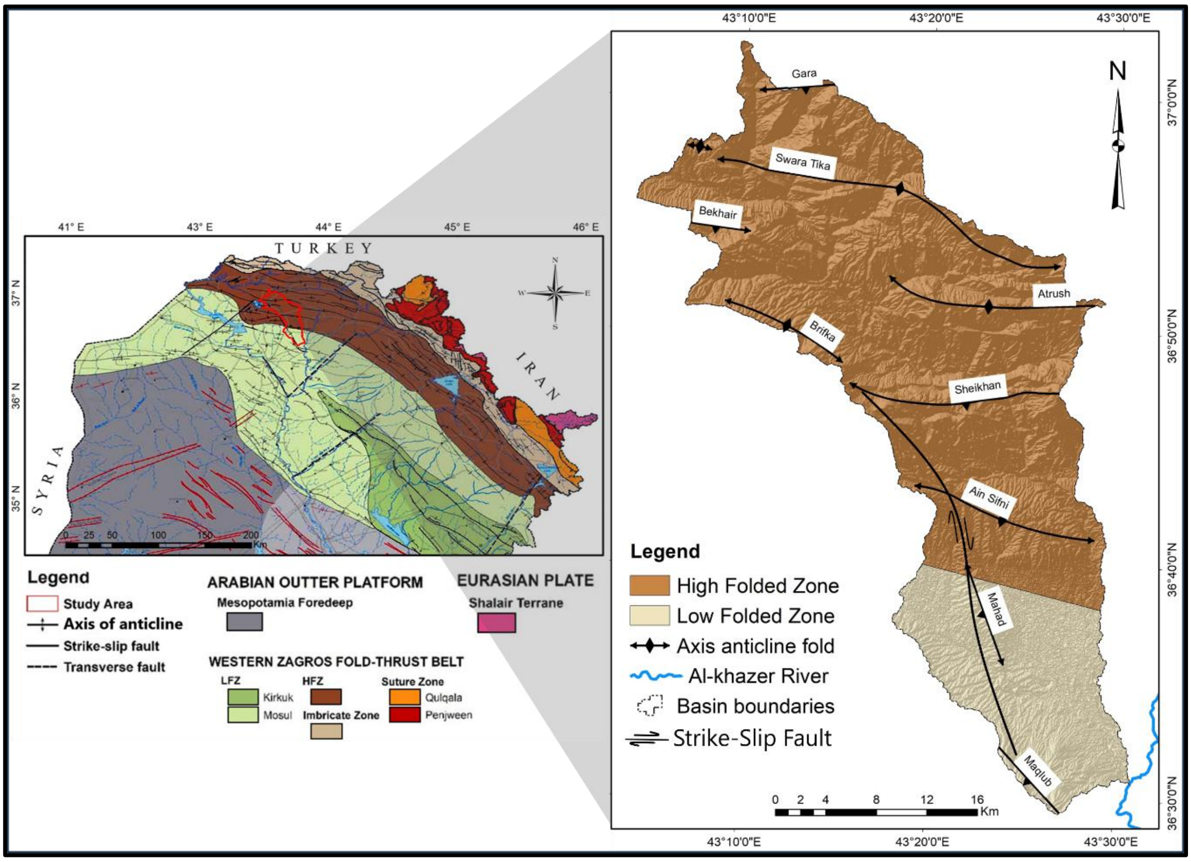

Figure 3: Tectonic division map of the study area (Fouad, 2015).

4.2. Stratigraphy

Geological formations are among the most important natural factors affecting the morphotectonics and geomorphology of the basin. Factors such as rock nature, layered structure system, and rock structures including faults, joints, and cracks interact with other factors in forming topographic characteristics. The geological history of the region may be limited to the Tertiary geological period and Quaternary deposits. The spatial distribution features of these formations can be traced in Figure 4 and Table 2, with formations plotted from oldest to youngest, summarized from Bellen (Bellen, 1959).

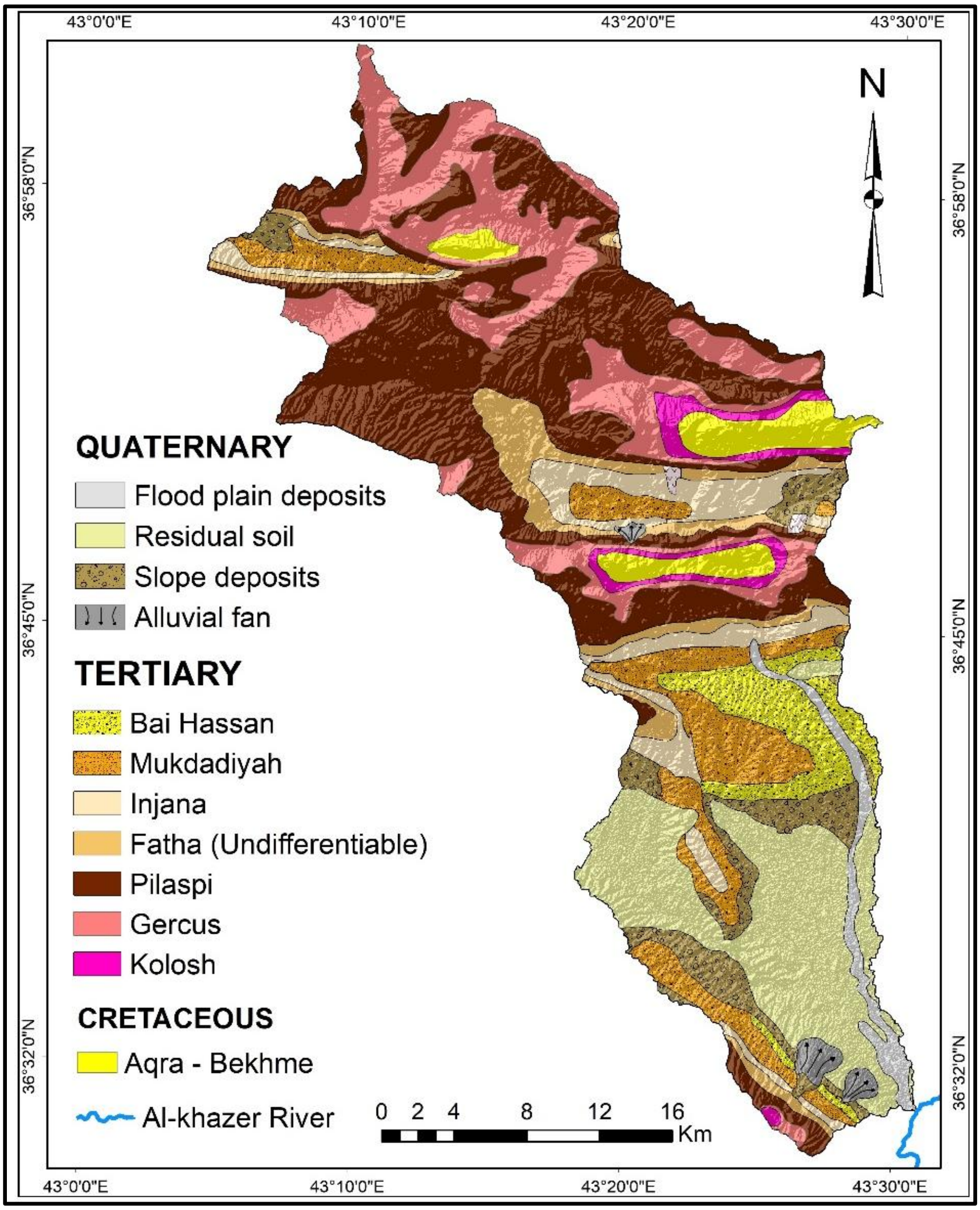

Figure 4: Geological map of the study area (Sissakian et al., 1995).

Table 2: The geological formation of the study area.

No.	Period	Formations	Geological age	Lithology	Km^2	%
1	Quaternary	Flood plain deposits	Holocene - Pleistocene	A mixture of sediments consisting of gravel, sand, clay, and silt.	18.67	1.99
2		Residual soil			129.37	13.84
3		Slope deposits			52.48	5.61
4		Alluvial fan			8.43	0.9
5	Neogene	Bai Hassan	Pliocene – Pleistocene.	Conglomerate, sandstone, claystone.	43.8	4.68
6		Mukdadiyah	L. Miocene – Pliocene.	Sandstone, siltstone, claystone.	89.45	9.57
7		Injana	L. Miocene.	sandstone	63.93	6.84
8		Fatha	M. Miocene.	Limestone, marl, gypsum	54.52	5.83
9	Paleogene	Pilaspi	L. Eocene	Limestone.	268.45	28.7
10		Gercus	M. Eocene	Claystone, sandstones, conglomerates.	145.35	15.55
11		Kolosh	L. Paleocene	Sandstone, claystone	21.06	2.25
12	Cretaceous	Aqra - Bekhme	Campanian – Maastrichtian	Limestones	39.7	4.24
			Total		935.21	100

5. Structures accompanying Strike-Slip Faults

In some cases, mountain belts (including the Zagros Fold Thrust Belt, where the study area is located) include major dextral or sinistral strike-slip faults. The locations of these faults are indicated on structural and geological maps of folded areas by the deviation or twisting of adjacent fold axes along the fault zone (Figure 5). Additionally, some structures appear that do not coincide with the main folds in the folded area, such as convex folds with axes deflected away from the main fold axes, usually inverted due to thrusting and uplifting displacement added to the strike-slip displacement within the strike-slip fault zone, with the appearance of pull-apart basins in the form of topographic depressions within the zone and other topographically elevated areas represented by isolated fault blocks (Horsetail splay).

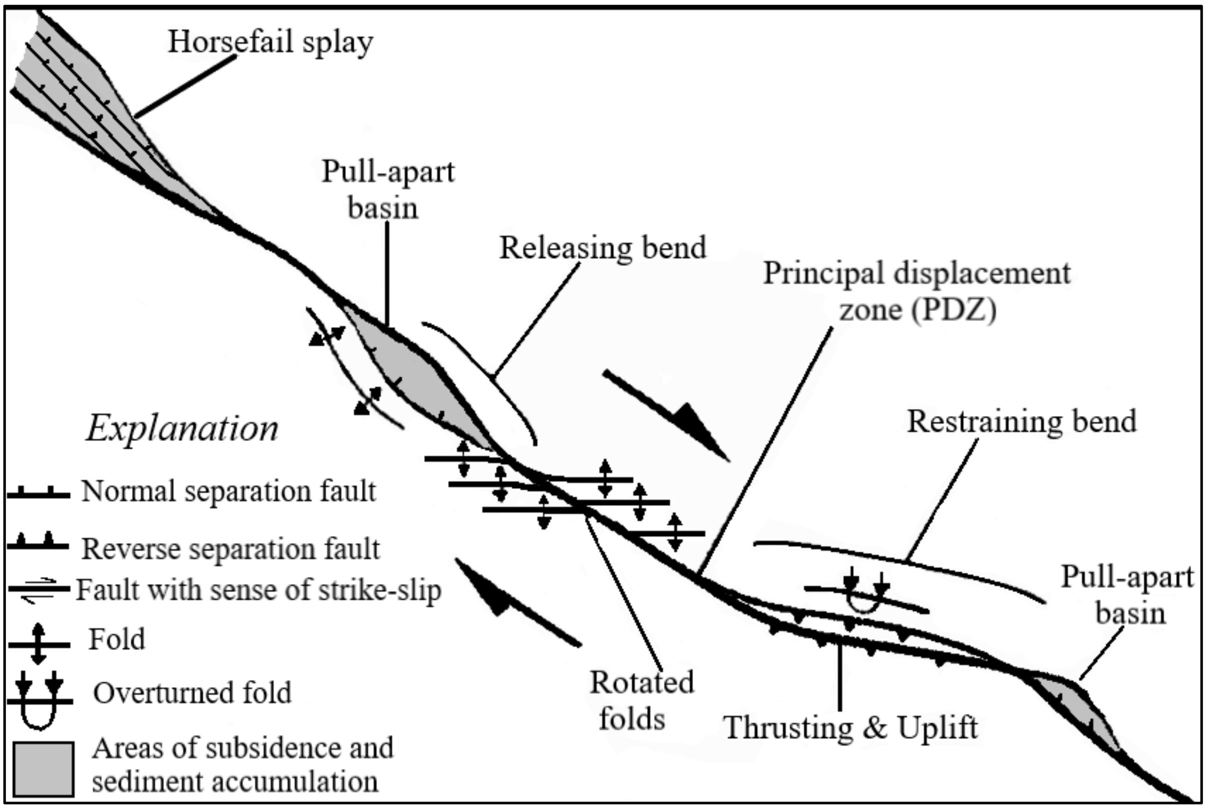

Figure 5: Important distinctive structures of the strike-slip fault zone in the structural map (modified from Burbank & Anderson, 2008).

6. Results

The current study developed a structural map of the study area using a geological map of northern Iraq (Sissakian et al., 1995) at a scale of 1:250,000 and a tectonic map (Fouad, 2015). A Digital Elevation Model of the study area was also utilized. After drawing the map and comparing it with Figure 5, the study identified a large dextral strike-slip fault. Its rightward movement caused the deviation of fold axes and separated some of them into eastern and western parts. In addition to this deviation and separation, the fault's movement also established a counterclockwise rotation of the two parts of the area. This caused the fold axes within the eastern part to generally rotate counterclockwise, resulting in some axes aligning approximately east-west (Figure 6a).

The southern part of the fault was identified and first recorded by Fouad (2012) and extends from the Maqloub to the Sheikhan anticline (Figure 3). Two other studies by Al-Moadhen et al. (2025) and Balaki (1991) reached the same conclusion. In our current study, we extended this fault from the Sheikhan Fold to the Swara Tika Fold based on our results.

6.1. Digital Elevation Model (DEM)

The study area is located between an elevation of 312 meters at the mouth of the basin and 1590 meters above sea level in the northeast of the basin. Elevation characteristics reflect the nature of tectonic movements and uplift and subsidence processes resulting from plate collision, which are confined to the basin's earth layers, in addition to external processes such as erosion and weathering (Al-Kanani, 2022; Figure 6b).

6.2. Drainage Basin Delineation And Stream Network Extraction

Using the Digital Elevation Model layer with 12.5 m resolution, two primary layers, stream vector layers and drainage basins, were extracted using the ArcGIS 10.3 program (Figure 6c). The DEM data were processed using hydrology tools in ArcGIS, and 38 sub-basins were identified (Figure 6d) along with stream networks (Taesiri et al., 2020). The extracted layers were used for matching with the basin Structural map.

6.3. Lineament Structures

Lineaments are linear or curved features (Pandey et al., 2023) and essential components for determining the earth's surface structures (Kumar et al., 2018) and morphological features, in addition to indicating deformation intensity (Yadav & Singh, 2022). Linaments play a pivotal role in revealing surface features; their characteristics are determined according to the distribution of structural and morphological features, drainage network pattern, textural variation, and lithological variations. (Morelli & Piana, 2006; Pal et al., 2006). (Figure 6e) shows the map of lineament structures extracted automatically using PCI Geomatica software.

6.4. Active Tectonics Index (IAT)

Five geomorphological indices were used to calculate the relative tectonic activity index (IAT) (Table 2). This categorization provides comprehensive information about all parameters affected by geomorphological tectonic activity in the research area. The Relative Tectonic Activity Index (IAT) is obtained by calculating the arithmetic mean of each class of geomorphological indices.

IAT values are grouped into four classes to determine the level of active tectonic relativity: class 1: very high ($1 < IAT \leq 1.5$); class 2: high ($1.5 < IAT \leq 2$); class 3: moderate ($2 < IAT \leq 2.5$); and class 4: low ($2.5 < IAT$) (El Hamdouni et al., 2008; Eynoddin et al., 2017) (Table 3) (Figuer 6f).

Table 3: IAT classes of Active Tectonic Index in the study area basin.

No. Sub-basin	T	AF	SMF	SL	VF	S	N	N/IAT=S	Class	Degree
1	3	3	1	3	3	13	5	2.6	4	Low active
2	3	1	1	3	3	11	5	2.2	3	Moderate active
3	1	1	1	3	3	9	5	1.8	2	High active
4	1	3	1	3	1	9	5	1.8	2	High active
5	2	2	1	3	3	11	5	2.2	3	Moderate active
6	3	3	1	3	3	13	5	2.6	4	Low active
7	2	3	1	3	3	12	5	2.4	3	Moderate active
8	1	3	1	3	2	10	5	2	2	High active
9	3	3	1	3	3	13	5	2.6	4	Low active
10	2	3	1	3	3	12	5	2.4	3	Moderate active
11	2	1	1	3	3	10	5	2	2	High active
12	3	3	1	3	3	13	5	2.6	4	Low active
13	3	3	1	3	3	13	5	2.6	4	Low active
14	3	3	1	3	3	13	5	2.6	4	Low active
15	1	3	1	3	3	11	5	2.2	3	Moderate active
16	3	3	1	3	3	13	5	2.6	4	Low active
17	2	3	1	3	2	11	5	2.2	3	Moderate active
18	3	3	1	3	2	12	5	2.4	3	Moderate active
19	2	3	1	3	2	11	5	2.2	3	Moderate active
20	2	1	1	3	3	10	5	2	2	High active
21	2	3	1	3	2	11	5	2.2	3	Moderate active
22	2	3	1	3	3	12	5	2.4	3	Moderate active
23	3	3	1	3	1	11	5	2.2	3	Moderate active
24	2	1	1	3	1	8	5	1.6	2	High active
25	3	2	1	3	3	12	5	2.4	3	Moderate active
26	1	3	1	3	3	11	5	2.2	3	Moderate active
27	1	3	1	3	3	11	5	2.2	3	Moderate active
28	1	3	1	3	3	11	5	2.2	3	Moderate active
29	1	3	1	3	3	11	5	2.2	3	Moderate active
30	2	3	1	3	3	12	5	2.4	3	Moderate active
31	3	3	1	3	3	13	5	2.6	4	Low active
32	2	3	1	3	3	12	5	2.4	3	Moderate active
33	2	3	1	3	3	12	5	2.4	3	Moderate active
34	1	2	1	3	3	10	5	2	2	High active
35	2	1	1	3	3	10	5	2	2	High active
36	1	3	1	3	3	11	5	2.2	3	Moderate active
37	3	3	1	3	3	13	5	2.6	4	Low active
38	1	3	1	3	3	11	5	2.2	3	Moderate active

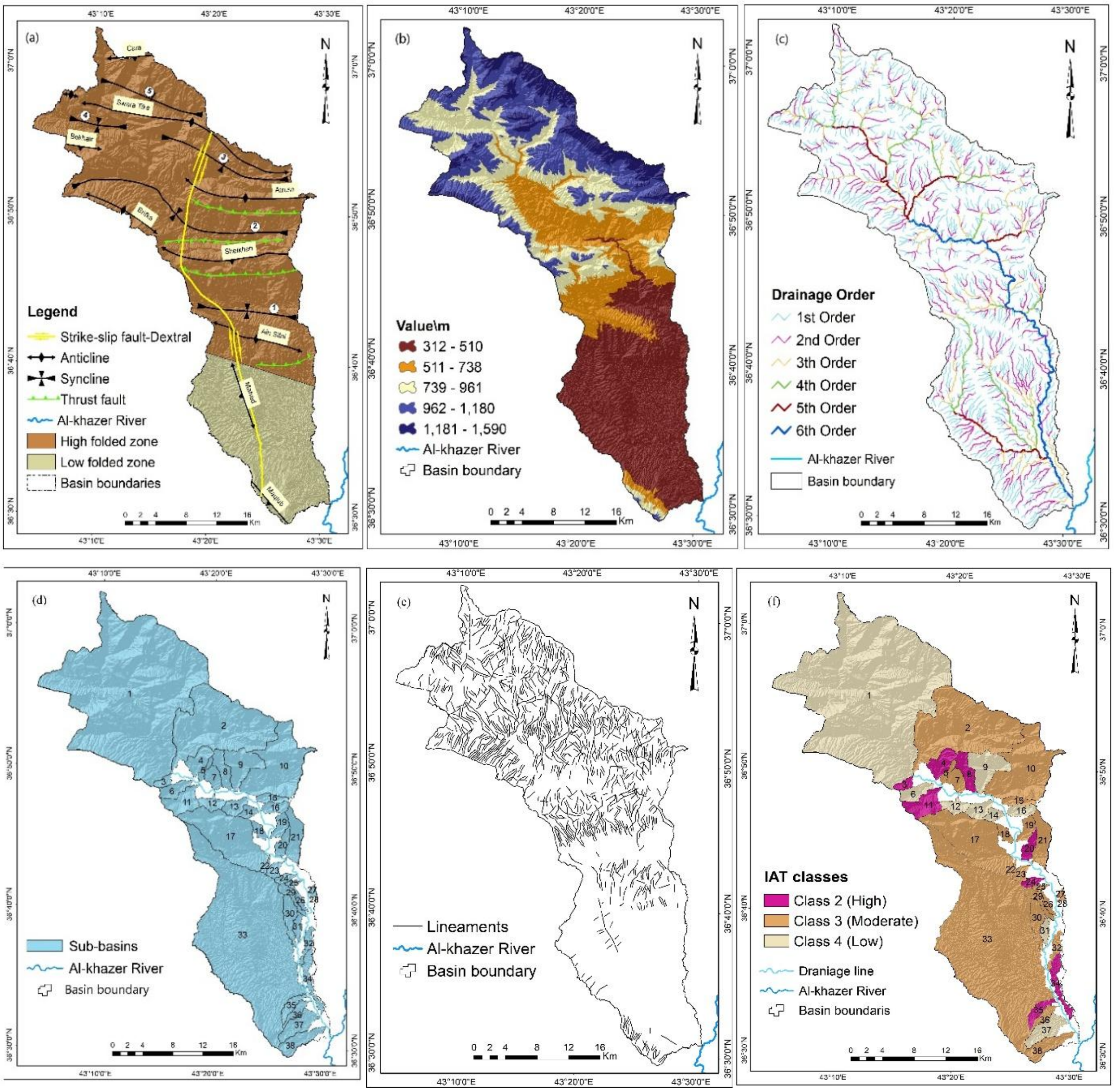

Figure 6: a) Structural map, b) Elevation map, c) stream network, d) Sub-basins, e) Lineaments, and f) Active Tectonics Index of the Gumal basin.

7. Structural Controlling for Folds and Faults in the Study Area

7.1. Fold and Fault Control on Basin Topography

The structural map clearly reflects the influence of the basin's topography, which has significantly contributed to elevation differences through the presence of folds distributed throughout the basin (Figure 7a).

This elevation variation is due to increased amplitude and development of the folds, particularly in the High Fold Zone, and the presence of thrust faults associated with the folds. A group of the core folds (Gara, Swara Tika, Bekhair, Brifka, and Atrush) exhibited the highest recorded elevation, at 1,590-1,181 meters above sea level within the High Fold Zone. Their area is

80.36 km², representing 8.59% of the total, which is the lowest percentage among all categories with steep slopes.

Elevations gradually decrease towards the southern part of the basin, reaching the Low Fold Zone, where the lowest recorded elevation was 510-312 meters, with an area of 306.67 km² representing 32.8%. This category constitutes the largest part of the basin area and is concentrated in the Low Fold Zone. The difference between the High Fold Zone and the Low Fold Zone through matching of the geological structures map and topographic map indicates limited tectonic uplift and fewer structures represented by folds within the Low Fold Zone.

7.2. Fold and Fault Control on Rock Outcrop Distribution

By matching the structural map with the geological map (Figure 7b), Cretaceous formations (specifically the Aqra-Bekhme Formation) are exposed in the cores of anticlines (Sawar Tika, Atrush, and Sheikhan) located in the northern part of the basin, within the High Fold Zone. In contrast, Tertiary formations are exposed only within the cores of anticlines in the southern part of the basin, within the Low Fold Zone. This indicates increased displacement and development of reverse faults associated with folds in the High Fold Zone compared to the Low Fold Zone.

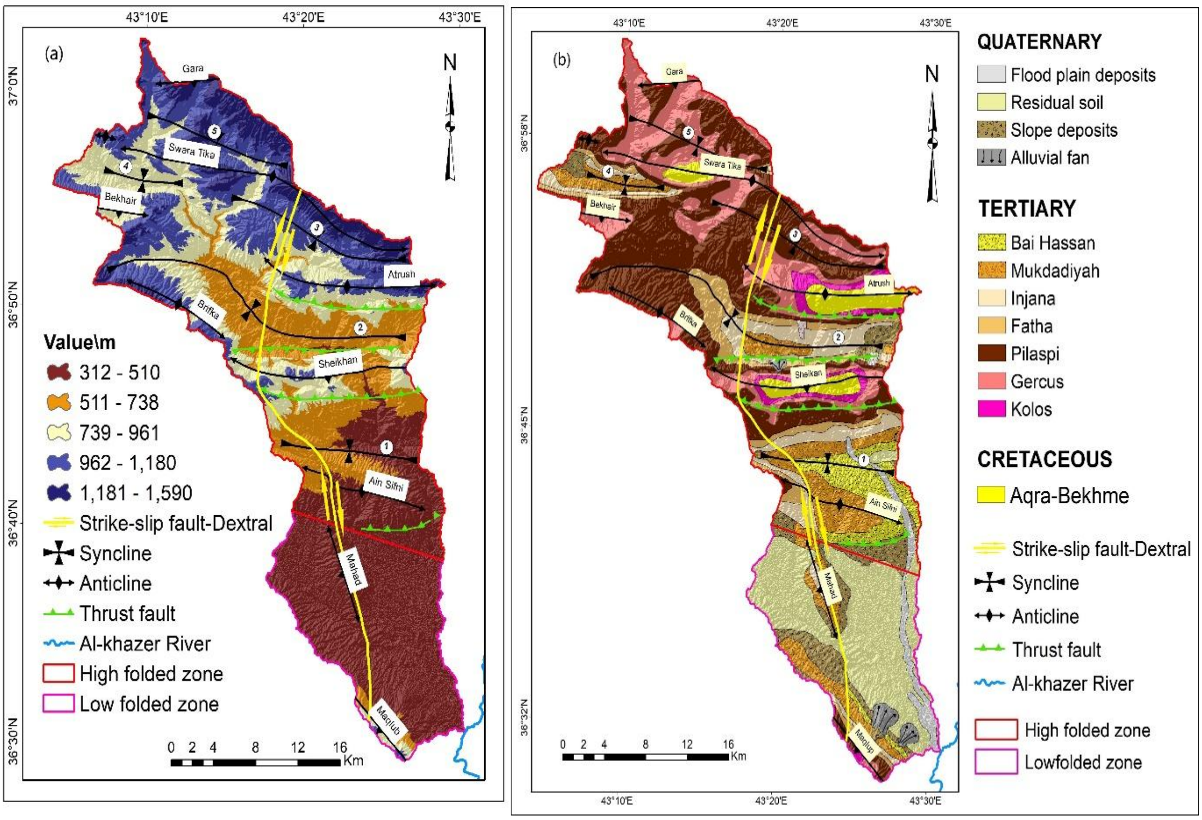

Figure 7: Fold and fault control map of the (a) topography and (b) geological map.

Regarding the low folds, some synclinal folds (3 and 5) show exposures of the highly rigid Pilaspi Formation alongside the Gercus Formation. These exposures occupy a large area within the high fold range, amounting to 267.85 km² (28.67%) and 145.35 km² (15.55%), respectively. The largest area is concentrated in the western part of the basin. This suggests that the amount of tectonic uplift in those areas was small compared to the eastern parts of the basin (Figure 7b).

This variation in area provides evidence of increased movement and development of thrust faults associated with folds located in the eastern part of the High Fold Zone (Atrush and Sheikhan folds). It also serves as evidence for the separation of the eastern part from the western part by a dextral strike-slip fault. The fault's rightward displacement increases the activity of reverse faults associated with the anticlines, thereby increasing the number of folds and uplifting the right block (Bertotti, 2004).

7.3. Fold and Fault Control on Stream Network

A matching map of the structural map with the stream network map of the study area showed that the basin boundaries are controlled and defined by folds and faults (Figure 8a). It is noted that the Gara and Swara Tika folds mark the northern and northeastern borders of the basin, the southern border is defined by the Maqlub fold, and the western border is defined by the Brifka and Bekhair folds. The eastern border is defined by the Al-Khazir River, which roughly coincides with the transverse Hadr Bakhma Fault, confirmed through geophysical data as a fault penetrating the basement rocks (Jassim & Goff, 2006).

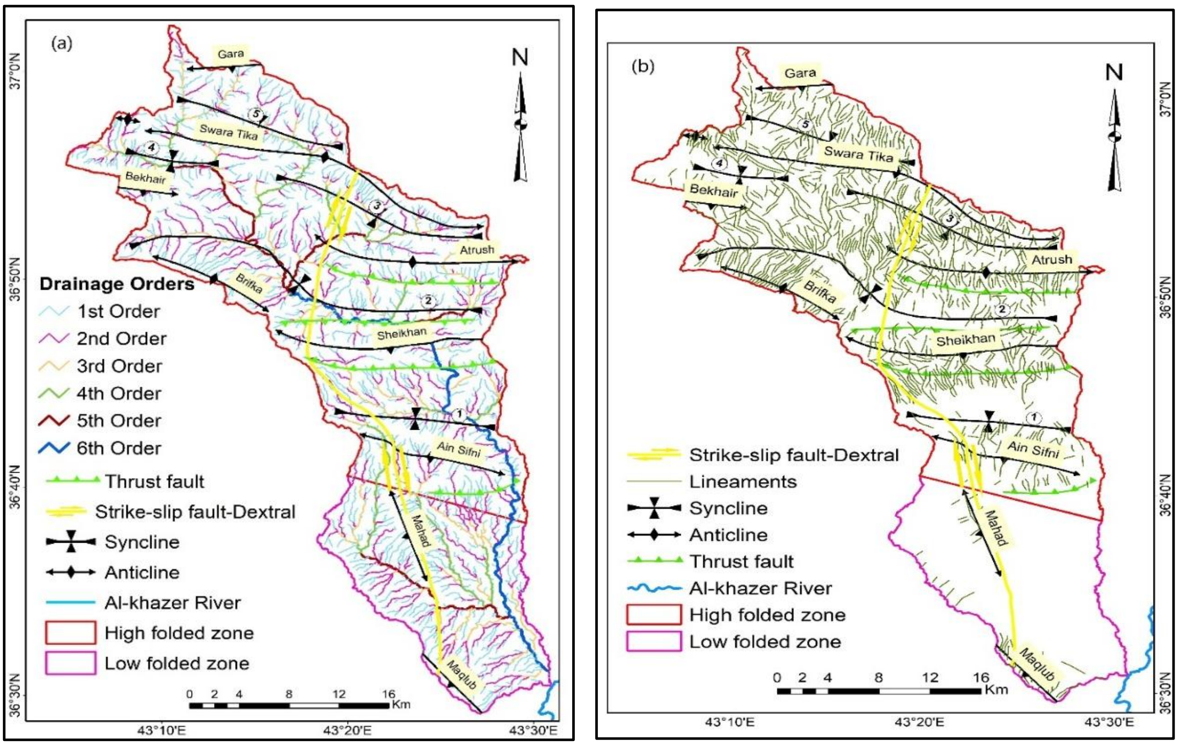

Figure 8: Fold and fault control map of the (a) Drainage and (b) Lineaments map.

Regarding the surface runoff network within the basin, the matching map also indicates that drainage patterns and river ranks within the basin vary between parallel, dendritic, centripetal, radial, and rectangular. This diversity is linked to the variety of rock exposures interspersed within the network, in addition to the distribution of synclinal and undulating folds. There is an ideal match of anticline axes with water divide lines, which confirms the role of anticlines in directing water network flow, in addition to determining the shape and boundaries of the basin. (Clevis, 2003) stated that the first orders of the water network gather along anticline axes as the beginning of drainage, while synclinal folds appear as water collection lines, usually with high river orders represented by rivers flowing within the area of the front limb of anticlines (the limb with the highest inclination).

7.4. Fold and Fault Control on Lineament Structure Distribution

The consistency of the structural map with the lineament structure map reveals the role of folds and faults in controlling the basin (Figure 8b). Lineament structures are densely distributed in areas on either side of anticline fold axes, which represent the cores of anticlines within the High Fold Zone (typically the Aqra-Bekhme Formation). This is attributed to the lithology of the exposed formations, which mainly consist of limestone. This limestone exhibits brittle behavior under tectonic stress, resulting in fractures that often serve as water drainage lines due to being weak areas. Furthermore, the erosion-resistant Pilaspi limestone formation occupies the largest area of the basin within the High Fold Zone. In the southern part of the basin, the density of lineament structures is low within the exposed areas of both the Ain Sifni Fold and the Mahad fold. This may be attributed to the fact that the exposed formations (Bai Hassan and Mukdadiyah) primarily consist of thick layers of compacted sediments, making them relatively fracture-free.

7.5. Fold and Fault Control on Sub-basins

The matching between the structural map and the secondary basin map, which contains 38 sub-basins, revealed that fold axes played an important role in dividing the secondary basins (Figure 9a). The large area of basin No. 1 compared to other basins may be attributed to the weak activity of thrust faults within the northeastern part of the basin, consistent with the movement of the dextral strike-slip fault that extends from north to south of the basin. Basin No. 33, which ranks second in terms of area and is located east of the Mahad anticline within the southern part of the basin, may be attributed to the scarcity of folds and their limited development, consistent with its location within the Low Fold Zone. Notably, small-area basins are found in high concentrations in the eastern part of the basin, providing clear evidence that their presence is linked to the abundance of anticlines and the counterclockwise deviation of their axes, moving closer to the east-west direction due to the dextral strike-slip fault extending from north to south of the basin.

7.6. Fold and Fault Control on Active Tectonics Index (IAT)

Matching the structural map with the Active Tectonics Index (IAT) map revealed the extent to which folds and faults influence the distribution of tectonic activation within the basin (Figure 9b). The upper basin areas, specifically the northeastern part, exhibited moderate to high tectonic activation compared to the rest of the basin, indicating reactivation and development of faults in those areas. This activation and development are reflected in the increased number of anticline folds resulting from the movement and development of associated faults. The northwestern parts of the basin exhibit less tectonic activity. For instance, the sub-basin located north of the basin, defined by the Gara and Brifka folds, shows low activity despite its location within the High Fold Zone. This has been attributed to the movement of the dextral strike-slip fault occurring at the expense of thrust fault activity in that area.

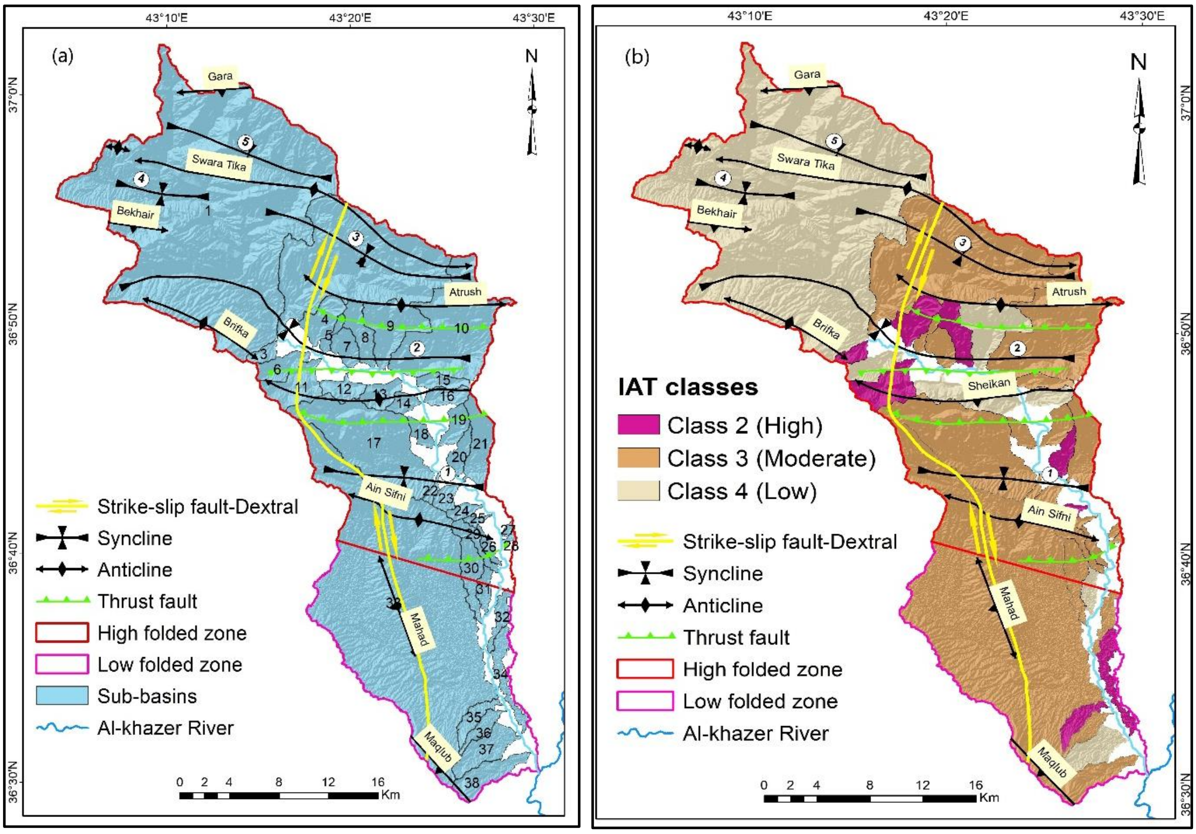

Figure 9: Fold and fault control map of the (a) Sub-basin and (b) Active Tectonics Index map.

8. Discussions

Matching the structural map with maps of topography, rock exposures, stream network, lineament structures, sub-basins, and Active Tectonics Index (IAT) (Figure 10) clearly showed that geological structures (folds and faults) played a significant role in shaping the basin's boundaries and distributing its topography and formation exposures. They also had a major role in distributing drainage patterns and dividing the stream network into sub-basins. Furthermore, dextral strike-slip faults play a major role in the Gumal Valley basin, cutting and terminating anticlines (Berberian, 1995). The structural map showed a dextral strike-slip fault extending from north to south in the study area. The movement of this fault caused the eastern part of the basin to advance southward in response to tectonic stress prevailing in northern Iraq. This led to its increased development compared to the western part, shown by an increase in the number of anticlines and a counterclockwise deviation of their axes, making them closer to an east-west orientation. This is clearly evidenced by the concentration of high and medium tectonic activity in the east and its decrease in the western part of the study area (Figure 9b).

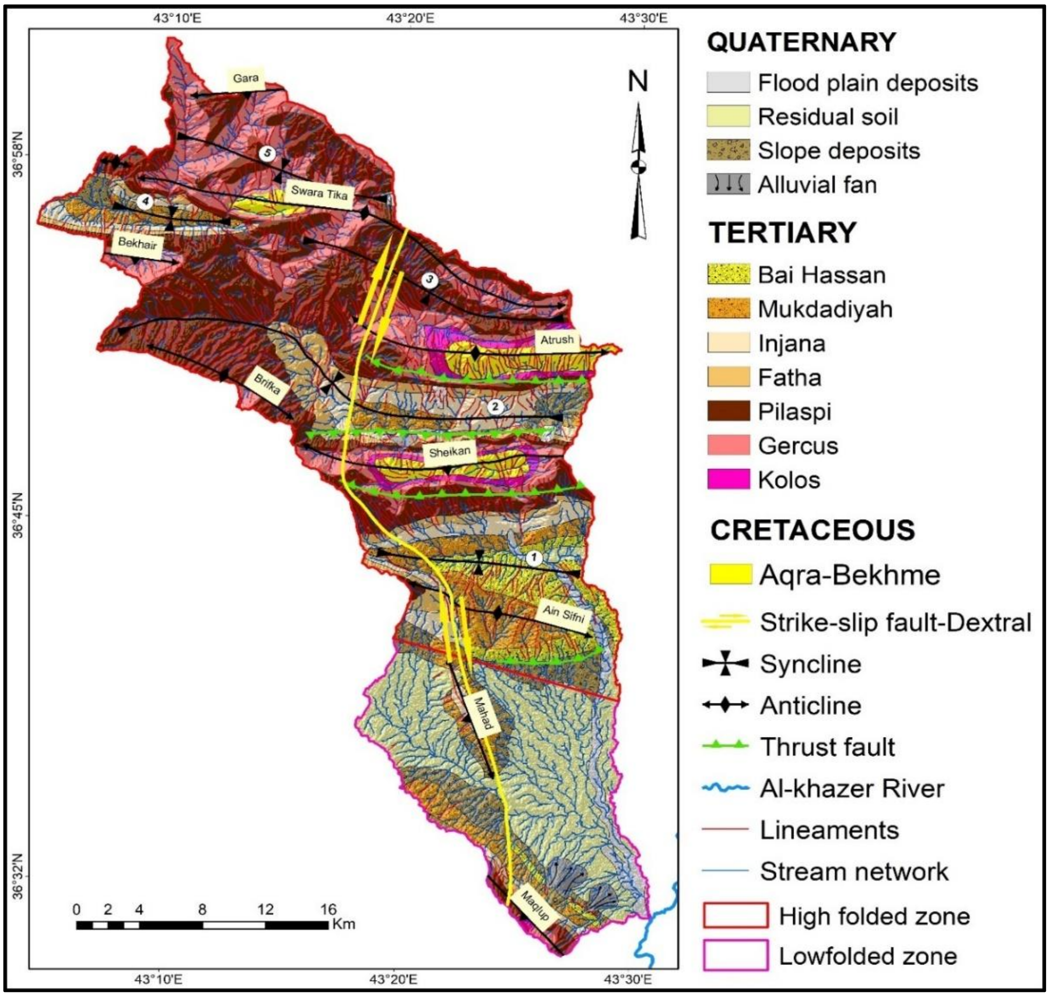

Figure 10: Assembled map to illustrate the role of geological structures in the distribution of rock exposures, surface runoff network, and lineament structures.

Although (Figure 10) shows that the study area (Gumal Basin) is part of the High and Low Fold Zones of the Western Iraqi Zagros belt, its northern part (within the High Fold Zone) is characterized by anticlines with Cretaceous formation exposures from the Mesozoic Era in their cores (Atrush and Sheikhan folds, with a small part of the Swara Tika fold). This reflects large displacements in faults related to the folds. In contrast, the southern part, within the Low Fold Zone, is characterized by low anticlines with Cenozoic formation exposures, reflecting diminishing movement of related faults. This is consistent with Numan (Numan, 1997 & 2000), who stated that the Late Cretaceous period witnessed tectonic reversal between the Arabian and

Eurasian (Iranian and Turkish) plates. This transformation from a divergent tensional phase to a compressional phase led to uplift and folding of the sedimentary cover in northern and northeastern Iraq. (Al-Azzawi, 2003) confirmed this by stating that fold development increases with aging towards the north and northeast, towards the convergence zone.

Regarding lineament structures, their presence is consistently dominant within brittle-behaving rock exposures (Pilaspi and Aqra-Bekhme formations). Furthermore, they are compatible with the surface flow network, especially with first-order streams, which are often located within erosion-resistant Pilaspi and Aqra-Bekhme formations.

9. Conclusion

The IAT results revealed that no basin was classified as Category 1 (very high activity). The study classified 21%, 55%, and 24% of basins as Categories 2 (high activity), 3 (medium activity), and 4 (low activity), respectively. The structural map showed a dextral strike-slip fault extending north-south in the study area. The movement of this fault caused the eastern part of the basin to advance southward in response to tectonic stress prevailing in northern Iraq. The current basin shape results from harmonized movement and reactivation of faults in the study area in response to compressive tectonic stress accompanying convergence and collision of the Eurasian and Arabian plates. The area is generally affected by moderate to high modern tectonic activity according to the results obtained by applying geomorphological indices equations.

References

Al-Azzawi, N. Q. (2003). The structural development of folds shape in the foreland belt of Iraq and its tectonic implications. *Unpublished Ph.D Thesis, Mosul University, Iraq*.

Al-Kanani, D. M. M. (2022). Geomorphology and Hydrology of the Valley Al-Talil Basin, Northeast of Maysan Governorate. *Master's Thesis, College of Education, University of Wasit, Iraq*.

Al-Kraaey, N. A. K. (2013). The effects of the lineaments phenomenon and its geomorphology are evidenced in the Allas fold / north Hamereen. *, Master's Thesis, Department of Geography, University of Tikrit College of Education, Tikrit, Iraq.*

Al-Moadhen, A. A. H., Khagoory, F. K., & Hasan, M. I. (2025). Faults Geometry and the Evolution of Ain Sifni Anticline, Northern Iraq. *The Iraqi Geological Journal*, 96–108.

Al-Shamaa, A. M. (1986). A tectonic study of the Al-Jazeera region in Iraq. *Master's Thesis, College of Science, University of Baghdad, Iraq.*

Balaki, H. G. (2019). Structural Evolution of the Bradost, Pirs, Berat, and Maqloub-Barda Rash Anticlines in the Zagros Fold Thrust Belt, Kurdistan Region, NE Iraq. Unpublished PhD. Thesis, Salahaddin University-Erbil, Erbil, Iraq. P 241.

Bellen, R., D. H. W. R., and M. D. (1959). Lexique statigraphique international, Vol. III, Iraq, Asia. *Engineering*, 333–333.

Berberian, M. (1995). Master "blind" thrust faults hidden under the Zagros folds: active basement tectonics and surface morphotectonics. *Tectonophysics*, *241*(3–4), 193–224.

Bertotti, G., B. S., R. P., and S. G. (2004). Bollettino di Geofisica. *International Journal of Earth Sciences, Vol. 45 - N. 1.*

Bull, W. B., McFadden, L. D., & Doehring, D. O. (1977). Geomorphology in arid regions. *Geomorphology in Arid Regions*.

Burbank, D. W. & Anderson, R. S. (2008). Tectonic Geomorphology. *Blackwell Science, Oxford*, 67–67.

Cheng, W., Wang, N., Zhao, M., & Zhao, S. (2016). Relative tectonics and debris flow hazards in the Beijing mountain area from DEM-derived geomorphic indices and drainage analysis. *Geomorphology*, *257*, 134–142.

Clevis, Q. (2003). Three-dimensional modelling of thrust controlled foreland basin stratigraphy. *Faculty of Earth Sciences, Utrecht University*.

Cox, R. T. (1994). Analysis of drainage-basin symmetry as a rapid technique to identify areas of possible Quaternary tilt-block tectonics: an example from the Mississippi Embayment. *Geological Society of America Bulletin*, *106*(5), 571–581.

Edward, K. A., & Nicholas, P. (2002). *Active tectonics: earthquakes, uplift, and landscape*. New Jersey: Prentice Hall.

El Hamdouni, R., Irigaray, C., Fernández, T., Chacón, J., & Keller, E. A. (2008). Assessment of relative active tectonics, southwest border of the Sierra Nevada (southern Spain). *Geomorphology*, *96*(1–2), 150–173.

Eynoddin, E. H., Solgi, A., Pourkermani, M., Matkan, A., & Arian, M. (2017). Assessment of relative active tectonics in the Bozgoush basin (SW of Caspian Sea). *Open Journal of Marine Science*, *7*(2), 211–237.

Fouad, S. F. A. (2012). Western Zagros fold–thrust belt, part I: The low folded zone. *Iraqi Bulletin of Geology and Mining*, *5*, 39–62.

Fouad, S. F. A. (2015). Tectonic map of Iraq, scale 1: 1000 000, 2012. *Iraqi Bulletin of Geology and Mining*, *11*(1), 1–7.

Hack, J. T. (1957). *Studies of longitudinal stream profiles in Virginia and Maryland* (Vol. 294). US Government Printing Office.

Jassim, S. Z., & Goff, J. C. (2006). *Geology of Iraq*. DOLIN, sro, distributed by Geological Society of London.

Jeong, S.-H., Oh, J.-S., & Kim, Y.-S. (2022). Evaluation Method of Tectonic Activity Using Geomorphic Indices and Its Applicability. *Journal of The Korean Geomorphological Association*, *29*(4), 85–103.

Kumar, N., Singh, S. K., & Pandey, H. K. (2018). Drainage morphometric analysis using open-access earth observation datasets in a drought-affected part of Bundelkhand, India. *Applied Geomatics*, *10*(3), 173–189.

Morelli, M., & Piana, F. (2006). Comparison between remote sensed lineaments and geological structures in intensively cultivated hills (Monferrato and Langhe domains, NW Italy). *International Journal of Remote Sensing*, *27*(20), 4471–4493.

Numan, N., & Azzawi, N. (1993). Structural and geotectonic interpretation of vergence directions of anticlines in the foreland folds of Iraq.

Numan, N. M. S. (1997). A plate tectonic scenario for the Phanerozoic succession in Iraq. *Iraqi Geological Journal*, *30*(2), 85–110.

Numan, N. M. S. (2000). Major Cretaceous tectonic events in Iraq. *Rafidain Journal of Science*, *11*(3), 32–52.

Pal, S. K., Majumdar, T. J., & Bhattacharya, A. K. (2006). Extraction of linear and anomalous features using ERS SAR data over the Singhbhum Shear Zone, Jharkhand, using the fast Fourier transform. *International Journal of Remote Sensing*, *27*(20), 4513–4528.

Pandey, H. K., Singh, V. K., Singh, S. K., & Sharma, S. K. (2023). Mapping and validation of groundwater dependent ecosystems (GDEs) in a drought-affected part of Bundelkhand region, India. *Groundwater for Sustainable Development*, *23*, 100979.

Partabian, A., Nourbakhsh, A., & Ameri, S. (2016). GIS-based evaluation of geomorphic response to tectonic activity in Makran Mountain Range, SE of Iran. *Geosciences Journal*, *20*(6), 921–934.

Sissakian, K. Varoujan, Hagopian. H. Dikran, Hasan. A. Eman. (1995). Geological Map of Iraq (Al- Mosul Quarter NJ – 38-13), 1; 250000, *1st Edition, State Establishment of Geological Survey and Mining, Baghdad, Iraq.*

Taesiri, V., Pourkermani, M., Sorbi, A., Almasian, M., & Arian, M. (2020). Morphotectonics of Alborz Province (Iran): A case study using GIS method. *Geotectonics*, *54*(5), 691–704.

Yadav, S. K., & Singh, S. K. (2022). Morpho-tectonic assessment of Central Northern escarpment of Peninsular India, based on tectonically sensitive geomorphic indices. *Physical Geography*, *43*(6), 753–783.

About the authors

Dr. Ayyed Hussein Ward, Ph.D. (Baghdad University, Baghdad, Iraq). Field of Interest: structural geology, Neo-tectonic, tectonic-stratigraphy, tectonic-geomorphology. Field of work: Lecturer in the specialty of geology (structural geology, structural analysis, geotectonic, field geology) for 12 years.

e-mail: aiedwarid@tu.edu.iq

Dr. Najm A. Kamel Al-Karai, Department of Applied Earth Sciences, College of Science, Tikrit University, Saladin, Iraq, Specialization: Physical Geography/ Applied Geomorphology, B.Sc. Baghdad University, 1999, M.Sc. University of Tikrit, 2013.Ph.D. (University of Tikrit), Iraq. Research interest (geomorphology/ remote sensing applications/ geographic information systems applications/ hydrology).

e-mail: najimalabdula@tu.edu.iq

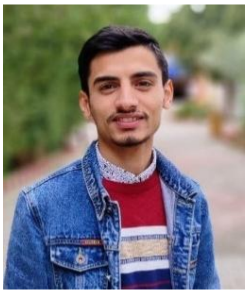

Mosab N. Al-Bana: graduated from the University of Mosul, Department of Earth Sciences, with a Bachelor’s degree in 2022, and is studying for a Master’s degree in Geomorphology and Structural Sciences at Tikrit University - College of Science - Department of Applied Earth Sciences.

e-mail: mosabjabber@gmail.com